α-$Ag_{2-2x}Zn_xWO_4$ ($0 \leq x \leq 0.25$) Solid Solutions: Structure, Morphology, and Optical Properties

Paula F. S. Pereira,[†] Clayane C. Santos,[‡] Amanda F. Gouveia,[‡] Mateus M. Ferrer,[§] Ivo M. Pinatti,[‡] Gleice Botelho,[‡] Julio R. Sambrano,[§] Ieda L. V. Rosa,[‡] Juan Andrés,[||] and Elson Longo[†]

[†]CDMF, LIEC, São Paulo State University (UNESP), P.O. Box 355, Araraquara 14800-900, Brazil

[‡]CDMF, LIEC, Federal University of São Carlos (UFSCar), P.O. Box 676, São Carlos 13565-905, Brazil

[§]Modeling and Molecular Simulations Group, São Paulo State University (UNESP), P.O. Box 473, Bauru 17033-360, Brazil

[||]Department of Analytical and Physical Chemistry, University Jaume I (UJI), Castelló 12071, Spain

Supporting Information

Photoluminescence: The α-Ag_2WO_4 crystals consist of [WO_6] and [AgO_y] (y = 2, 4, 6, and 7) clusters in the lattice; thus, the [WO_6] clusters are linked by strong bonds [–W–O–W–] between the clusters, resulting in internal vibrational spectra that provide information on the structure and order-disorder effects in the framework. If a symmetry break occurs, it can induce the formation of different structures with different properties and, consequently, can modify the electronic levels of the materials and significantly influence the PL emission properties.

In general, it is assumed that the PL emissions of metal tungstates are related to the charge-transfer transitions within the distortions in tetrahedral [WO_4] clusters or are due to oxygen vacancies or surface defects.[1,2] Thus, this cluster-to-cluster charge transfer (CCCT) process in the α-Ag_2WO_4 crystals is characterized by excitations involving electronic transitions between the distorted $[WO_6]_o^x$–$[WO_6]_d^x$ and $[AgO_y]_o^x$–$[AgO_y]_d^x$ (y = 2, 4, 6, and 7) clusters.[1-3] The blue–green emission of tungstate is due to

the charge transfer transitions within the [WO_6] cluster, and the emission in the red region is likely due to the [AgO_y] (y = 2, 4, 6, and 7) clusters, which form vacancies, inducing more disorder and deeper defects in the forbidden band gap; thus, the PL emission peaks situated at longer wavelengths were related to deep-level defects due to distortions in the lattice modifier clusters [AgO_y] (y = 2, 4, 6, and 7).[2,4]

The PL emission behavior of α-$Ag_{2-2x}Zn_xWO_4$ can be explained through equations (1–4) below, according to the notation of Kröger–Vink.[5] The electron−hole (e′−h•) pairs can be created before the electrons achieve the system. The structural distortions in $[WO_6]_d^x$–$[AgO_y]_d^x$ (intrinsic defects) are able to polarize the structure and make electronic transitions between $[WO_6]_d^x$ / $[AgO_y]_d^x$ and $[WO_6]_o^x$ / $[AgO_y]_o^x$ (disordered and ordered neutral clusters, respectively). Thus, when the photon energy is finally absorbed by the crystal, electron transitions to the conduction band occur and, subsequently, the relaxation of the network causes photons to be emitted. The superscript x indicates neutral clusters, • present clusters with one hole (positive charge, $h^{\bullet}$), and $'$ indicates clusters with one electron (negative charge, e′).

$$[WO_6]_d^x + [WO_6]_o^x \rightarrow [WO_6]_d^{\bullet} + [WO_6]_o' \quad (1)$$

$$[AgO_y]_d^x + [AgO_y]_o^x \rightarrow [AgO_y]_d^{\bullet} + [AgO_y]_o' \quad (2)$$

$$[WO_6]_d^x + [AgO_y]_o^x \rightarrow [WO_6]_d^{\bullet} + [AgO_y]_o' \quad (3)$$

$$[AgO_y]_d^x + [WO_6]_o^x \rightarrow [AgO_y]_d^{\bullet} + [WO_6]_o' \quad (4)$$

The equations (1–4) show the formation of e′–$h^{\bullet}$ pairs in the α-Ag_2WO_4 lattice due to ordered and disordered $[WO_6]_d^x$ / $[WO_6]_o^x$, $[AgO_y]_d^x$ / $[AgO_y]_o^x$, and $[WO_6]_d^x$/$[AgO_y]_o^x$ neutral clusters, consequently promoting the blue–green emission, thus leading to the generation of shallow defects (see Figure 12) as explained above and expressed through equations (5) and (6).

$$[ZnO_y]_d^{\bullet} + [WO_6]_o' \rightarrow [ZnO_y]_o^x + [WO_6]_o^x \quad (5)$$

$$[ZnO_y]_d^{\bullet} + [AgO_y]_o' \rightarrow [ZnO_y]_d^x + [AgO_y]_o^x \quad (6)$$

The suppression of the blue–green emission occurs in equation (5), in which the $[WO_6]_o'$ clusters (donors) transfer their electrons to $[ZnO_y]_d^{\bullet}$ clusters (acceptors), resulting in neutral clusters. The $[ZnO_y]_d^{\bullet}$ new clusters act as network modifiers contributing to the recombination of e′–$h^{\bullet}$ pairs.

Tables

Table SI-1. X-ray fluorescence of the chemical analysis of zinc-doped in α-$Ag_{2-2x}Zn_xWO_4$ ($0.05 \leq x \leq 0.25$) obtained by CP method at 80 ºC for 30 min.

Samples	Theoretical (mol) for Ag^+	Experimental XRF (mol) for Ag^+	Theoretical (mol) for Zn^{2+}	Experimental XRF (mol) for Zn^{2+}
α-$Ag_{1.90}Zn_{0.05}WO_4$	1.90	1.98	0.05	0.08
α-$Ag_{1.80}Zn_{0.10}WO_4$	1.80	1.80	0.10	0.14
α-$Ag_{1.70}Zn_{0.15}WO_4$	1.70	1.83	0.15	0.18
α-$Ag_{1.60}Zn_{0.20}WO_4$	1.60	1.71	0.20	0.22
α-$Ag_{1.50}Zn_{0.25}WO_4$	1.50	1.44	0.25	0.28

Table SI-2. Lattice parameters, unit cell volume and statistical parameters of quality obtained by Rietveld refinement for the α-$Ag_{2-2x}Zn_xWO_4$ (x = 0, 0.05, 0.10, 0.15, 0.20 and 0.25 mol) microcrystals synthesized by CP method at 80 ºC for 30 min.

Refined formula (α-$Ag_{2-2x}Zn_xWO_4$)	Lattice Parameters			Cell volume ($Å^3$)	R_{Bragg} (%)	χ^2 (%)	R_{wp} (%)	R_p (%)
	a (Å)	b (Å)	c (Å)					
***x* = 0**	10.8868(5)	12.0399(7)	5.9071(1)	774.28(9)	1.78	1.90	9.83	7.73
***x* = 0.05**	10.8637(9)	12.0246(2)	5.8998(3)	770.71(4)	2.17	1.71	8.40	6.43
***x* = 0.10**	10.8660(5)	12.0286(0)	5.9005(2)	771.21(9)	1.57	1.77	8.57	6.37
***x* = 0.15**	10.8543(8)	12.0176(6)	5.8943(2)	768.88(2)	1.60	1.83	8.59	6.26
***x* = 0.20**	10.8502(6)	12.0190(6)	5.8953(1)	768.80(7)	2.23	2.09	9.71	7.50
***x* = 0.25**	10.8421(3)	12.0138(7)	5.8963(6)	768.03(8)	2.15	2.01	9.65	7.44
ICSD N° 4165	10.89(2)	12.03(2)	5.92(2)	775.56	-	-	-	-

Table SI-3. Atomic positions of the α-$Ag_{2-2x}Zn_xWO_4$ (x = 0, 0.05 and 0.10) samples.

Atom	α-$Ag_{2-2x}Zn_xWO_4$								
	***x* = 0**			***x* = 0.05**			**x = 0.10**		
	x	**y**	**z**	**x**	**y**	**z**	**x**	**y**	**z**
W1	0.2592(1)	-0.0054(5)	0.5233(4)	0.2564(9)	-0.0050(5)	0.5187(6)	0.2577(2)	-0.0039(5)	0.5228(3)
W2	0.000	0.8420(4)	0.500	0.000	0.8446(2)	0.500	0.000	0.8435(4)	0.500
W3	0.000	0.1325(4)	0.500	0.000	0.1397(4)	0.500	0.000	0.1340(4)	0.500
Ag1	0.7605(8)	0.1768(3)	0.9906(6)	0.7550(7)	0.1659(9)	0.9847(1)	0.7664(7)	0.1751(5)	0.9899(3)
Ag2	0.2445(8)	0.8233(3)	0.0121(6)	0.2380(8)	0.8168(3)	0.0137(5)	0.2504(7)	0.8216(5)	0.0114(3)
Ag3	0.000	0.9929(3)	0.000	0.000	0.9951(6)	0.000	0.000	0.9912(5)	0.000
Ag4	0.000	0.6588(3)	0.000	0.000	0.6591(7)	0.000	0.000	0.6571(5)	0.000
Ag5	0.000	0.3205(3)	0.000	0.000	0.3139(3)	0.000	0.000	0.3188(4)	0.000
Ag6	0.000	0.5149(3)	0.500	0.000	0.5084(2)	0.500	0.000	0.5132(5)	0.500
O1	0.3570(9)	0.5929(8)	0.1800(6)	0.3641(7)	0.5987(8)	0.1959(6)	0.3669(5)	0.6008(6)	0.1811(9)
O2	0.3570(9)	0.3589(8)	0.1730(6)	0.3796(4)	0.3781(1)	0.1703(2)	0.3669(5)	0.3668(6)	0.1741(9)
O3	0.4080(9)	0.7159(8)	0.8000(6)	0.4133(7)	0.7307(1)	0.8107(8)	0.4179(5)	0.7238(6)	0.8011(9)
O4	0.4140(9)	0.2439(8)	0.7770(6)	0.3863(2)	0.2747(4)	0.7945(7)	0.4239(5)	0.2518(6)	0.7781(9)
O5	0.1510(9)	0.4749(8)	0.2670(6)	0.1648(8)	0.4706(7)	0.2696(0)	0.1609(5)	0.4828(6)	0.2681(9)
O6	0.4030(9)	0.4769(8)	0.8320(6)	0.4158(4)	0.4827(7)	0.8439(1)	0.4129(5)	0.4848(6)	0.8331(9)
O7	0.1780(9)	0.5929(8)	0.8420(6)	0.1970(2)	0.6092(2)	0.8199(7)	0.1879(5)	0.6008(6)	0.8431(9)
O8	0.1820(9)	0.3599(8)	0.8850(6)	0.1919(1)	0.4081(4)	0.9378(1)	0.1919(5)	0.3678(6)	0.8861(9)
Zn1	-	-	-	-	-	-	0.7664(7)	0.1751(5)	0.9899(3)
Zn2	-	-	-	-	-	-	0.2504(7)	0.8216(5)	0.0114(3)
Zn3	-	-	-	-	-	-	0.000	0.9912(5)	0.000
Zn4	-	-	-	-	-	-	0.000	0.6571(5)	0.000
Zn5	-	-	-	-	-	-	0.000	0.3188(4)	0.000
Zn6	-	-	-	-	-	-	0.000	0.5132(5)	0.500

Table SI-4. Atomic positions of the α-$Ag_{2-2x}Zn_xWO_4$ (x = 0.15, 0.20 and 0.25) samples.

Atom	α-$Ag_{2-2x}Zn_xWO_4$								
	***x* = 0.15**			***x* = 0.20**			**x = 0.25**		
	x	**y**	**z**	**x**	**y**	**z**	**x**	**y**	**z**
W1	0.2576(2)	-0.0038(1)	0.5247(8)	0.2597(0)	0.0016(1)	0.5259(0)	0.2621(3)	0.0021(4)	0.5295(7)
W2	0.000	0.8436(8)	0.500	0.000	0.8491(1)	0.500	0.000	0.8496(4)	0.500
W3	0.000	0.1341(8)	0.500	0.000	0.1396(1)	0.500	0.000	0.1401(4)	0.500
Ag1	0.7674(6)	0.1748(9)	0.9892(5)	0.7464(5)	0.1694(1)	0.9896(2)	0.7458(2)	0.1688(3)	0.9879(8)
Ag2	0.2414(6)	0.8213(9)	0.0107(5)	0.2304(5)	0.8159(1)	0.0111(2)	0.2298(2)	0.8153(3)	0.0094(8)
Ag3	0.000	0.9909(5)	0.000	0.000	0.9855(1)	0.000	0.000	0.9849(3)	0.000
Ag4	0.000	0.6568(9)	0.000	0.000	0.6514(1)	0.000	0.000	0.6508(3)	0.000
Ag5	0.000	0.3185(9)	0.000	0.000	0.3131(1)	0.000	0.000	0.3125(3)	0.000
Ag6	0.000	0.5129(9)	0.500	0.000	0.5075(1)	0.500	0.000	0.5069(3)	0.500
O1	0.3679(8)	0.6047(2)	0.1767(7)	0.3760(7)	0.6209(7)	0.1777(4)	0.3803(6)	0.6249(7)	0.1757(3)
O2	0.3679(8)	0.3707(2)	0.1697(7)	0.3760(7)	0.3869(7)	0.1707(4)	0.3803(6)	0.3909(7)	0.1687(3)
O3	0.4189(8)	0.7277(2)	0.7967(7)	0.4270(7)	0.7439(7)	0.7977(4)	0.4313(6)	0.7479(7)	0.7957(3)
O4	0.4249(8)	0.2557(2)	0.7737(7)	0.4330(7)	0.2719(7)	0.7747(4)	0.4373(6)	0.2759(7)	0.7727(3)
O5	0.1619(8)	0.4867(2)	0.2637(7)	0.1700(7)	0.5029(7)	0.2647(3)	0.1743(6)	0.5069(7)	0.2627(3)
O6	0.4139(8)	0.4867(2)	0.8320(6)	0.4220(7)	0.5049(7)	0.8397(4)	0.4263(6)	0.5089(7)	0.8277(3)
O7	0.1889(8)	0.6047(2)	0.8420(6)	0.1970(7)	0.6209(7)	0.8397(4)	0.2013(6)	0.6249(7)	0.8377(3)
O8	0.1929(8)	0.3717(2)	0.8817(7)	0.2010(7)	0.3879(7)	0.8827(3)	0.2053(6)	0.3919(7)	0.8807(3)
Zn1	0.7674(6)	0.1748(9)	0.9892(5)	0.7464(5)	0.1694(1)	0.9896(2)	0.7458(2)	0.1688(3)	0.9879(8)
Zn2	0.2414(6)	0.8213(9)	0.0107(5)	0.2304(5)	0.8159(1)	0.0111(2)	0.2298(2)	0.8153(3)	0.0094(8)
Zn3	0.000	0.9909(5)	0.000	0.000	0.9855(1)	0.000	0.000	0.9849(3)	0.000
Zn4	0.000	0.6568(9)	0.000	0.000	0.6514(1)	0.000	0.000	0.6508(3)	0.000
Zn5	0.000	0.3185(9)	0.000	0.000	0.3131(1)	0.000	0.000	0.3125(3)	0.000
Zn6	0.000	0.5129(9)	0.500	0.000	0.5075(1)	0.500	0.000	0.5069(3)	0.500

Table SI-5. Raman modes (in cm^{-1}) of α-$Ag_{2-2x}Zn_xWO_4$ (x = 0, 0.05, 0.10, 0.15, 0.20 and 0.25) microcrystals obtained by the CP method at 80 ºC for 30 min, compared to the literature.

Mode	This work		Literature values			
	Experimental	Theoretical	Turkovic et al.[6]	Sreedevi et al.[7]	Pinatti et al.[8]	Longo et al.[9] (theo.)
A_{1g}	-	41.3	44	-	-	40.4
A_{1g}	60	61.3	60	70	59	54.1
B_{1g}	82	81.7	92	-	81	87.0
A_{2g}	116	116.1	116	103	114	112.2
A_{2g}	179	179.6	182	175	179	152.4
A_{1g}	206	205.7	208	205	204	212.4
B_{1g}	249	250.6	248	246	249	246.2
A_{2g}	306	304.9	306	301	301	308.6
B_{2g}	338	338.4	336	335	-	329.6
A_{2g}	368	369.4	366	361	365	369.5
B_{2g}	486	443.9	488	475	-	450.8
B_{2g}	508	456.7	510	504	-	523.4
B_{2g}	-	474.9	546	544	-	564.2
A_{1g}	586	620.0	590	588	584	599.4
B_{1g}	-	631.1	629	624	-	628.6
B_{1g}	669	668.8	667	664	662	662.8
B_{1g}	728	730.8	730	722	-	712.7
B_{2g}	759	753.5	754	742	755	716.6
A_{1g}	778	778.9	778	773	777	809.0
A_{2g}	805	798.2	800	791	801	813.5
A_{1g}	884	890.6	884	881	881	845.3

Captions for Figures

Figure SI-1. Magnification of region between 2θ = 29.5º to 34º.

Figure SI-2. XRD of α-$Ag_{2-2x}Zn_xWO_4$ where: (a) 0.30 (b) 0.35 (c) 0.40 and (d) 0.45 microcrystals, obtained by CP method at 80 ° C for 30 min.

Figure SI-3. Rietveld refinement plot for α-$Ag_{2-2x}Zn_xWO_4$ synthesized by the CP method at 80 ºC for 30 min: (a) x = 0, (b) x = 0.05, (c) x = 0.10, (d) x = 0.15, (e) x = 0.20, and (f) x = 0.25.

Figure SI-4. Theoretical models of α-$Ag_{2-2x}Zn_xWO_4$ with 25 % of Zn^{2+}.

Figure SI-5. FT-IR spectra of the α-$Ag_{2-2x}Zn_xWO_4$ (x = (a) 0, (b) 0.05, (c) 0.10, (d) 0.15, (e) 0.20 and (f) 0.25) microcrystals obtained by the CP method at 80 ºC for 30 min.

Figure SI-6. Map of morphologies of α-Ag_2WO_4 with (010), (100), (001) (110), (101), and (011) surfaces. Surface energy is expressed in J m^{-2}.

Figure SI-7. UV-Vis spectra for α-$Ag_{2-2x}Zn_xWO_4$ synthesized by the CP method at 80 ºC for 30 min: (a) x = 0, (b) x = 0.05, (c) x = 0.10, (d) x = 0.15, (e) x = 0.20, and (f) x = 0.25.

Figures

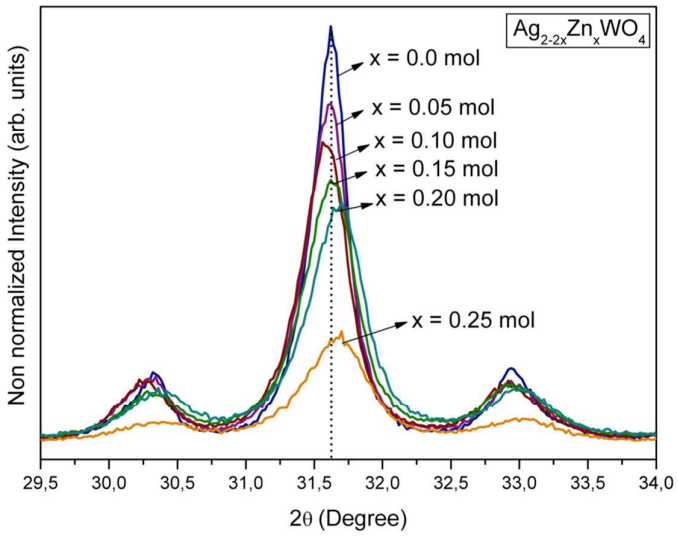

<Figure SI-1>

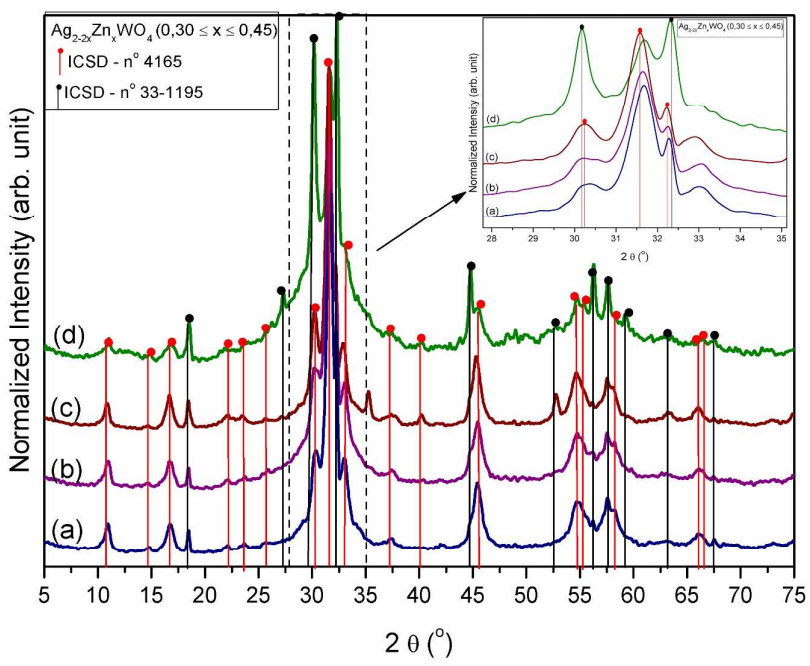

<Figure SI-2>

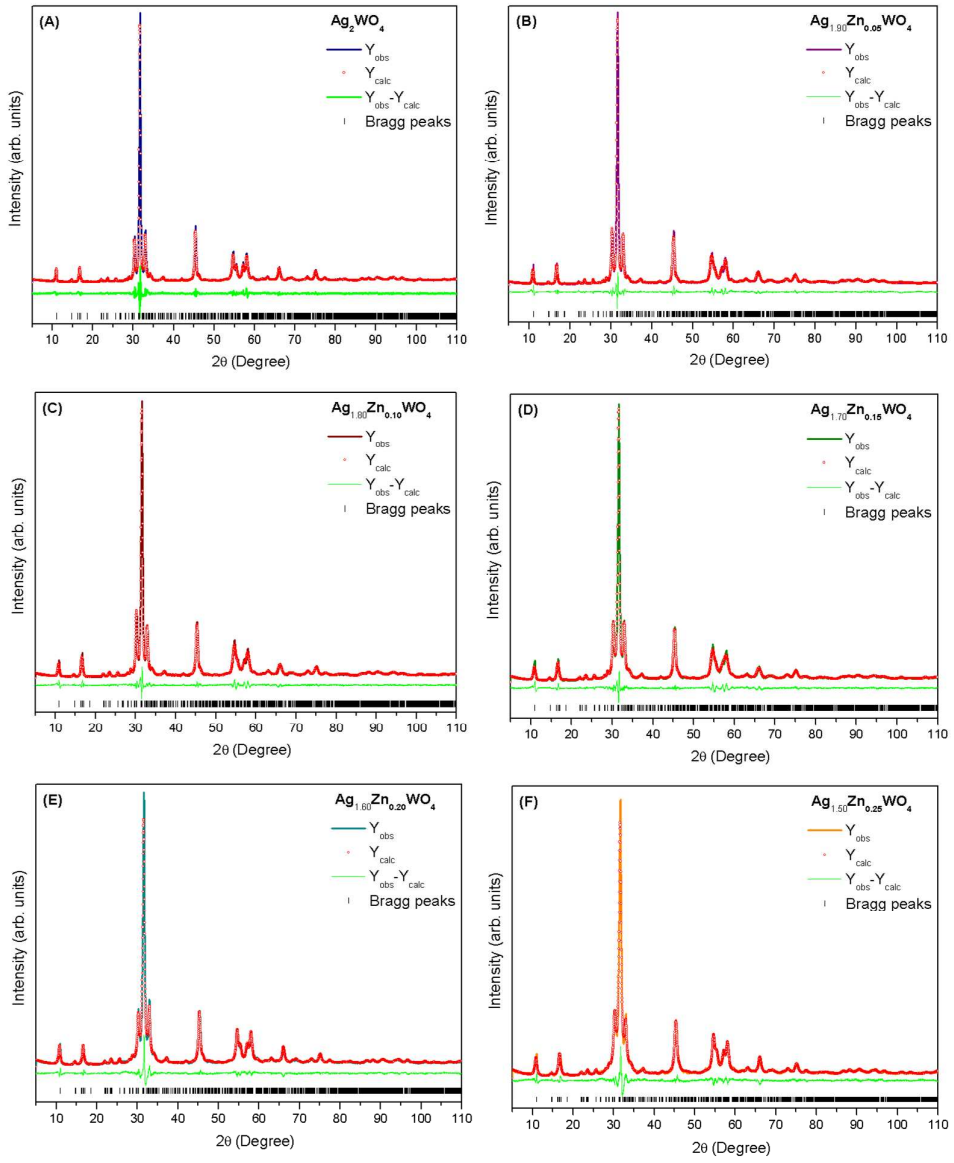
(A)
Ag2WO4
(B)
Ag1.90Zn0.05WO4
(C)
Ag1.80Zn0.10WO4
(D)
Ag1.70Zn0.15WO4
(E)
Ag1.60Zn0.20WO4
(F)
Ag1.50Zn0.25WO4
Yobs
Ycalc
Yobs-Ycalc
Bragg peaks
Intensity (arb. units)
2θ (Degree)

<Figure SI-3>

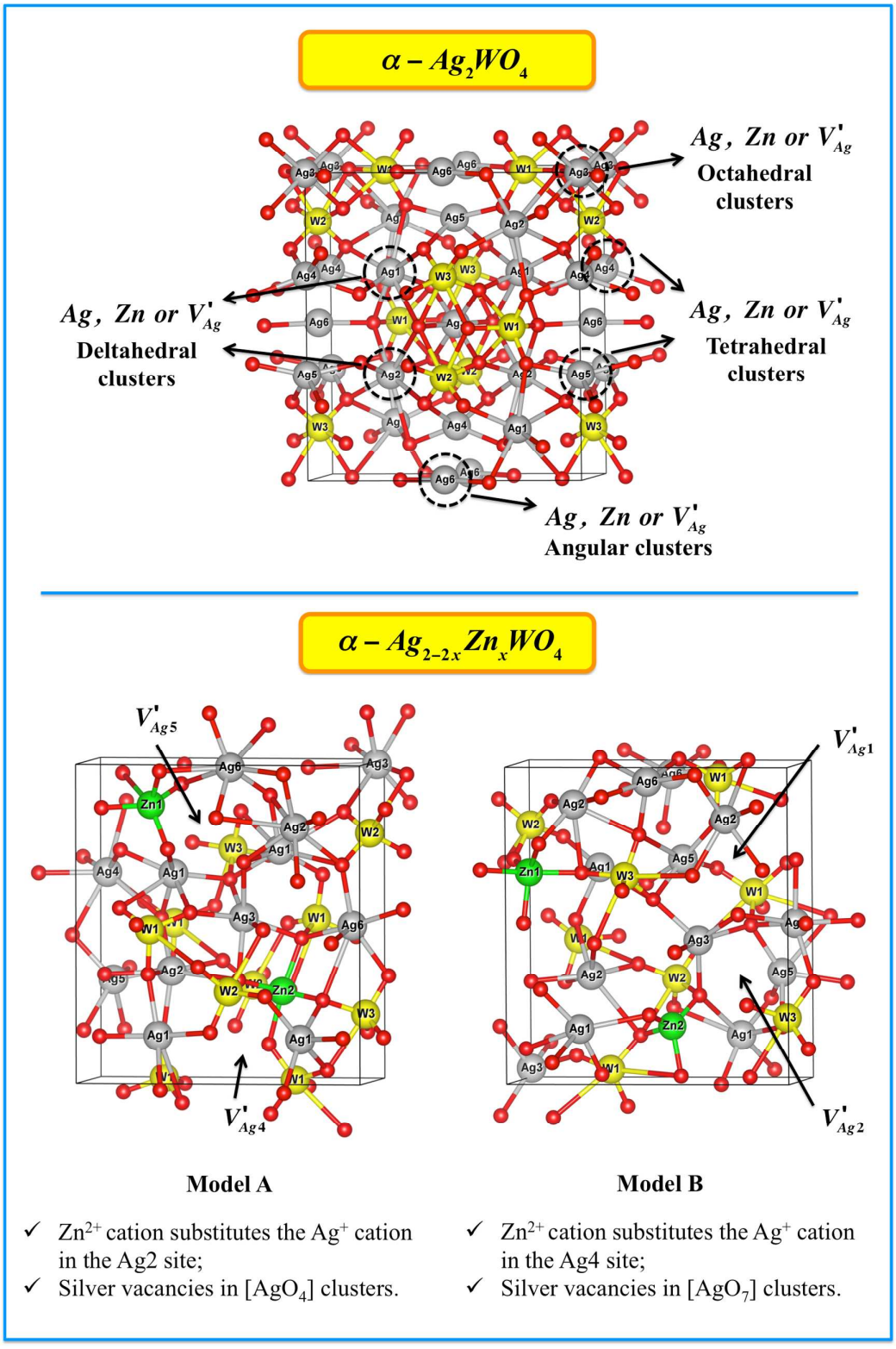
α – Ag2WO4
Ag, Zn or V'Ag
Octahedral clusters
Ag, Zn or V'Ag
Tetrahedral clusters
Ag, Zn or V'Ag
Deltahedral clusters
Ag, Zn or V'Ag
Angular clusters
α – Ag2-2xZnxWO4
V'Ag5
V'Ag4
V'Ag1
V'Ag2
Model A
Model B
✓ Zn2+ cation substitutes the Ag+ cation in the Ag2 site;
✓ Silver vacancies in [AgO4] clusters.
✓ Zn2+ cation substitutes the Ag+ cation in the Ag4 site;
✓ Silver vacancies in [AgO7] clusters.

<Figure SI-4>

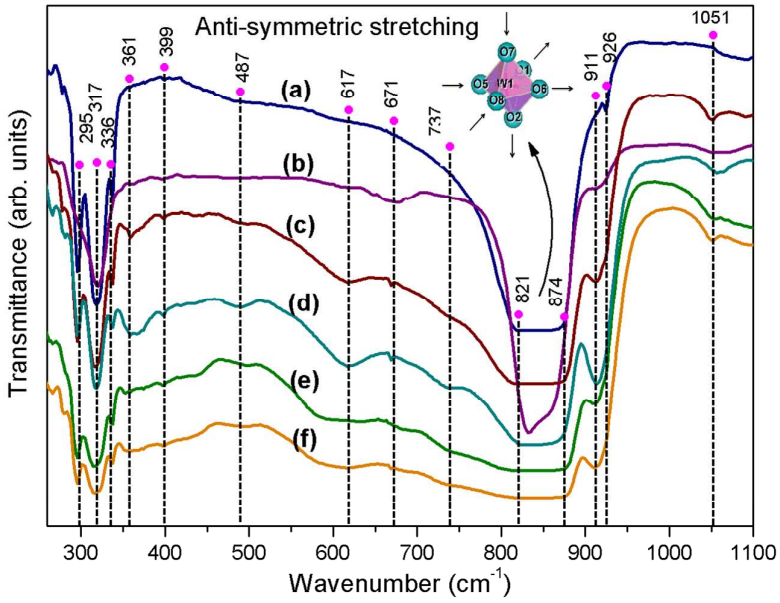

<Figure SI-5>

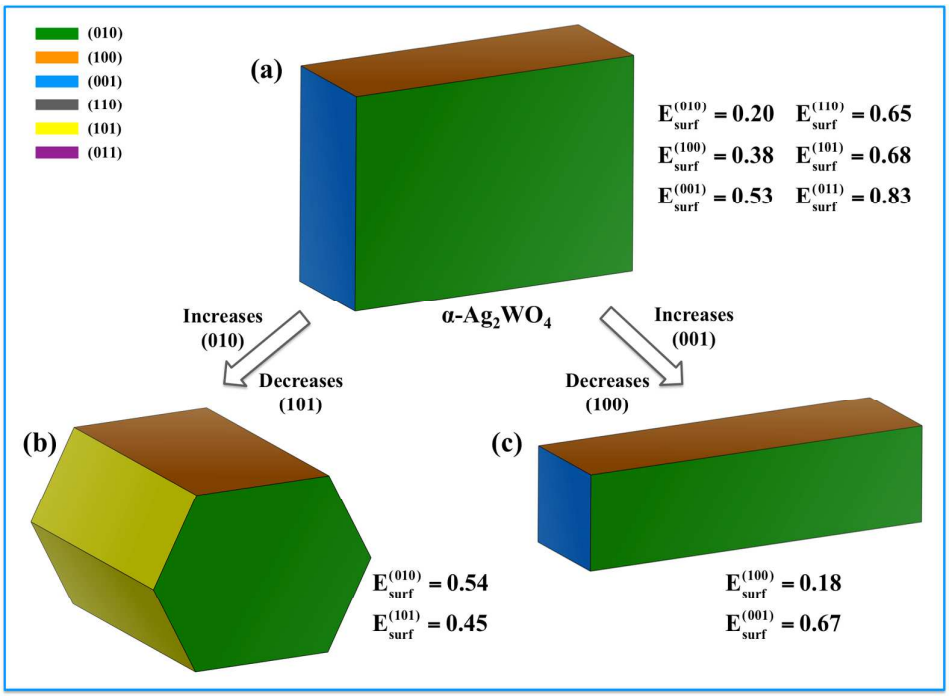

<Figure SI-6>

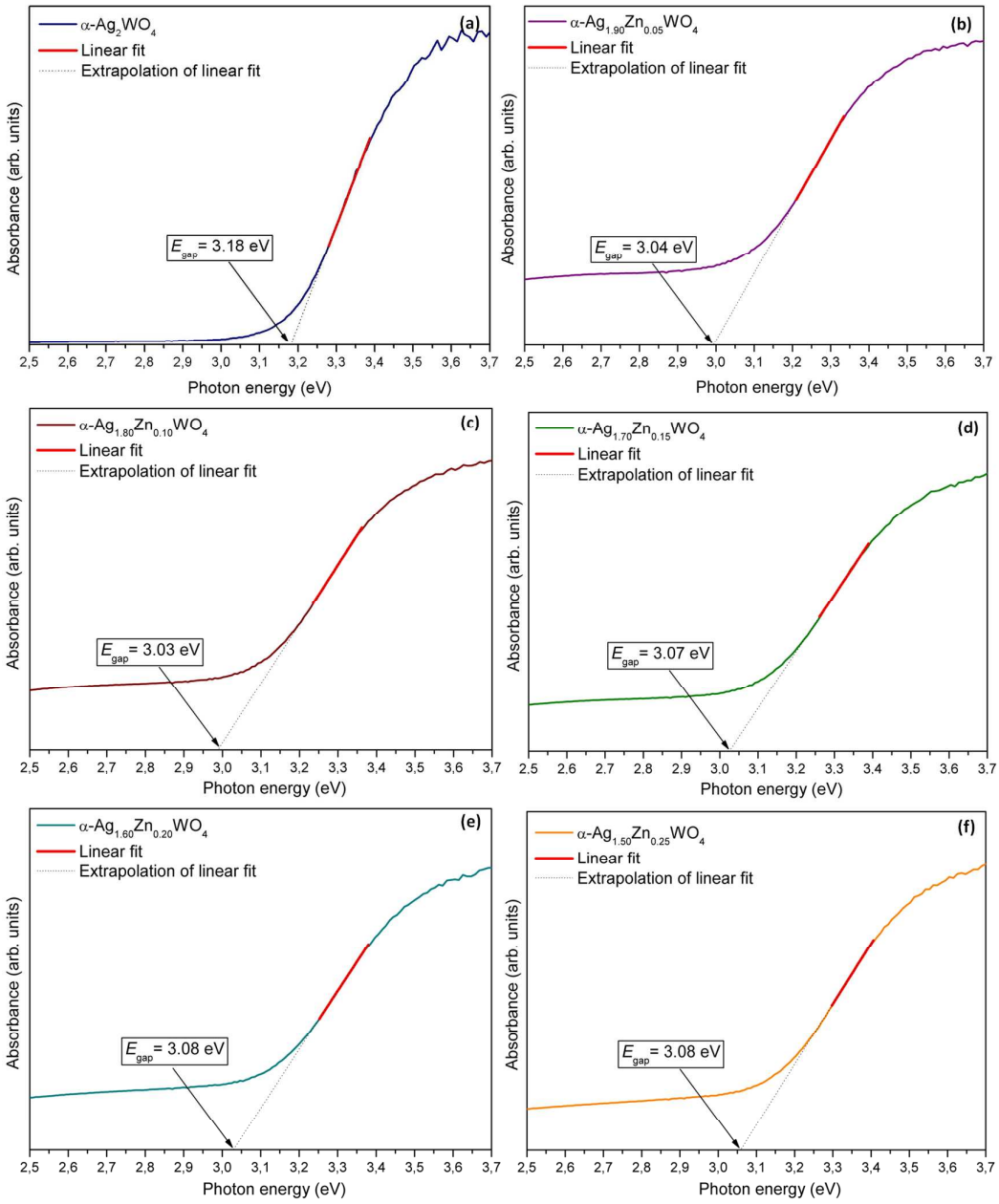
α-Ag2WO4
Linear fit
Extrapolation of linear fit
(a)
Egap = 3.18 eV
Absorbance (arb. units)
Photon energy (eV)
α-Ag1.90Zn0.05WO4
(b)
Egap = 3.04 eV
α-Ag1.80Zn0.10WO4
(c)
Egap = 3.03 eV
α-Ag1.70Zn0.15WO4
(d)
Egap = 3.07 eV
α-Ag1.60Zn0.20WO4
(e)
Egap = 3.08 eV
α-Ag1.50Zn0.25WO4
(f)
Egap = 3.08 eV

<Figure SI-7>

REFERENCES

(1) Gouveia, A. F.; Sczancoski, J. C.; Ferrer, M. M.; Lima, A. S.; Santos, M. R.; Li, M. S.; Santos, R. S.; Longo, E.; Cavalcante, L. S., Experimental and theoretical investigations of electronic structure and photoluminescence properties of beta-Ag2MoO4 microcrystals. *Inorg. Chem.* **2014,** *53*, 5589-99.

(2) Pereira, W. d. S.; Ferrer, M. M.; Botelho, G.; Gracia, L.; Nogueira, I. C.; Pinatti, I. M.; Rosa, I. L. V.; La Porta, F. d. A.; Andrés, J.; Longo, E., Effects of chemical substitution on the structural and optical properties of α-Ag2−2xNixWO4 (0 ≤ x ≤ 0.08) solid solutions. *Phys. Chem. Chem. Phys.* **2016,** *18*, 21966-21975.

(3) Cavalcante, L. S.; Almeida, M. A.; Avansi, W., Jr.; Tranquilin, R. L.; Longo, E.; Batista, N. C.; Mastelaro, V. R.; Li, M. S., Cluster coordination and photoluminescence properties of alpha-Ag2WO4 microcrystals. *Inorg. Chem.* **2012,** *51*, 10675-87.

(4) Longo, E.; Volanti, D. P.; Longo, V. M.; Gracia, L.; Nogueira, I. C.; Almeida, M. A. P.; Pinheiro, A. N.; Ferrer, M. M.; Cavalcante, L. S.; Andres, J., Toward an Understanding of the Growth of Ag Filaments on alpha-Ag2WO4 and Their Photoluminescent Properties: A Combined Experimental and Theoretical Study. *J. Phys. Chem. C* **2014,** *118*, 1229-1239.

(5) Kröger, F. A.; Vink, H. J., Relations between the Concentrations of Imperfections in Crystalline Solids. *Solid State Phys.* **1956,** *3*, 307-435.

(6) Turkovi, A.; Fox, D. L.; Scott, J. F.; Geller, S.; Ruse, G. F., High temperature raman spectroscopy of silver tetratungstate, Ag8W4O16. *Mat. Res. Bull.* **1977,** *12*, 189-196.

(7) Sreedevi, A.; Priyanka, K. P.; Babitha, K. K.; Aloysius Sabu, N.; Anu, T. S.; Varghese, T., Chemical synthesis, structural characterization and optical properties of nanophase α-Ag2WO4. *Indian J. Phys.* **2015,** *89*, 889-897.

(8) Pinatti, I. M.; Nogueira, I. C.; Pereira, W. d. S.; Pereira, P. F. S.; Gonçalves, R. F.; Varela, J. A.; Longo, E.; Rosa, I. L. V., Structural and photoluminescence properties of Eu3+ doped [small alpha]-Ag2WO4 synthesized by the green coprecipitation methodology. *Dalton Trans.* **2015,** *44*, 17673-17685.

(9) Longo, E.; Volanti, D. P.; Longo, V. M.; Gracia, L.; Nogueira, I. C.; Almeida, M. A. P.; Pinheiro, A. N.; Ferrer, M. M.; Cavalcante, L. S.; Andres, J., Toward an Understanding of the Growth of Ag Filaments on α-Ag2WO4and Their Photoluminescent Properties: A Combined Experimental and Theoretical Study. *J. Phys. Chem. C* **2014,** *118*, 1229-1239.